Building Upon Patterned Organic Monolayers Produced via Catalytic Stamp Lithography

Hidenori Mizuno and Jillian M. Buriak*

Department of Chemistry, University of Alberta, and the National Institute for Nanotechnology, Edmonton, Alberta, T6G 2G2 Canada

ABSTRACT Soft lithographic sub-100 nm chemical patterning was demonstrated on organic monolayer surfaces using poly(dimethylsiloxane)-based stamps decorated with Pd nanostructures, structures termed "catalytic stamps". Chemically reactive azide or alkene functionalities were incorporated on oxide-capped silicon surfaces and utilized for patterning via Pd-catalyzed hydrogenation or Heck reactions. The catalytic stamps were soft lithographic stamps based on PDMS with embedded nanoscale palladium catalysts, prepared via block copolymer-based templating. Nanoscale chemical patterns were readily generated on the azide or alkene precursor surfaces simply by applying the Pd catalytic stamps and the reactive molecule, the molecular ink, to the surface, thanks to the highly localized catalytic transformations induced by the patterned, immobilized solid Pd catalysts. A series of successful postfunctionalization reactions on the resulting patterned surfaces further demonstrated the utility of this approach to construct novel designs of nanoarchitectures, with potentially unique and innovative properties.

KEYWORDS: nanoscale patterning • organic monolayer • catalytic stamp • palladium • catalyst • hydrogenation • Heck reaction

INTRODUCTION

The demand for the creation of novel nanostructured materials is rapidly growing in a range of scientific and engineering communities (1). One of the foci of this trend is the exploration of unique and innovative properties that are potentially useful for emerging/existing technologies, such as molecular electronics (2), sensing (3), photovoltaics (4), bioengineering (5), and others. Construction of hybrid functional systems commonly requires the assembly of a variety of organic, inorganic, and biological building blocks onto host substrates, with defined orientation and alignment. Organic monolayer-based surface patterning provides a simple and versatile approach to this end, allowing rational and flexible designs of platforms in terms of resulting surface chemistries (6).

Considerable effort has been ongoing in recent years to improve and build upon the ability of various patterning techniques (1, 7−12). Efforts include, for example, parallel dip-pen nanolithography (7), polymer pen lithography (8), advanced soft lithography (i.e., topography-free (9), catalytic (10), or nano contact printing (11), etc.), and many others (12). In the case of contact printing, challenges include ink diffusion (13) and stamp deformation (14), both problems that must be overcome to regularly achieve sub-100 nm resolution, while maintaining high-throughput and large-area capabilities with low cost. Our approach toward this challenge has been the introduction of catalytic stamps, poly(dimethylsiloxane) (PDMS)-based stamps integrated with nanopatterned transition metal catalysts (15). Using these functional stamps, catalytic hydrosilylation of alkenes/alkynes/aldehydes was demonstrated on H-terminated Si surfaces, and molecular patterns with down to 15 nm resolution have been produced (15b).

In this work, we describe a new set of reactions applied to catalytic stamp-mediated sub-100 nm patterning of organic monolayers. Different from the previous hydrosilylation-based patterning, where molecular inks were delivered directly to inorganic (Si) interfaces (15), the patterning herein was achieved via the modification of preformed organic monolayers. Two different reactions, hydrogenation and the Heck reaction, were investigated using azide- and alkene-terminated oxide-capped Si surfaces, respectively. Subsequent functionalization of as-patterned surfaces and the reusability of catalytic stamps were also discussed.

RESULTS AND DISCUSSION

Catalytic stamps were fabricated through the two-step process as reported previously, an approach that involves the following two steps (15): (1) Synthesis of nanopatterned Pd catalysts on solid supports using self-assembled block copolymer templates. (2) Transfer of the Pd onto the surfaces of PDMS stamps by peeling-off. Three types of a commercially available family of block copolymers, polystyrene-*block*-poly-2-vinylpyridine, were utilized to create corresponding Pd catalytic stamps with different domain sizes (15−54 nm), center-to-center spacings (59−168 nm), and geometries (hexagonal or linear pattern) of catalysts (vide infra, Figures 1a, 4a, and 6a). Because the immobilized catalysts on PDMS have flat interfaces (15), intimate contact between the catalysts and substrates upon stamping is enhanced, as shown vide infra.

Two varieties of precursor surfaces on silicon, azide- and alkene-terminated, were prepared according to literature

* Corresponding author. E-mail: jburiak@ualberta.ca.
Received for review April 20, 2010 and accepted July 9, 2010

DOI: 10.1021/am100348f

Scheme 1. Outline for the Nanoscale Modification on Organic Monolayers Using Catalytic Stamps[a]

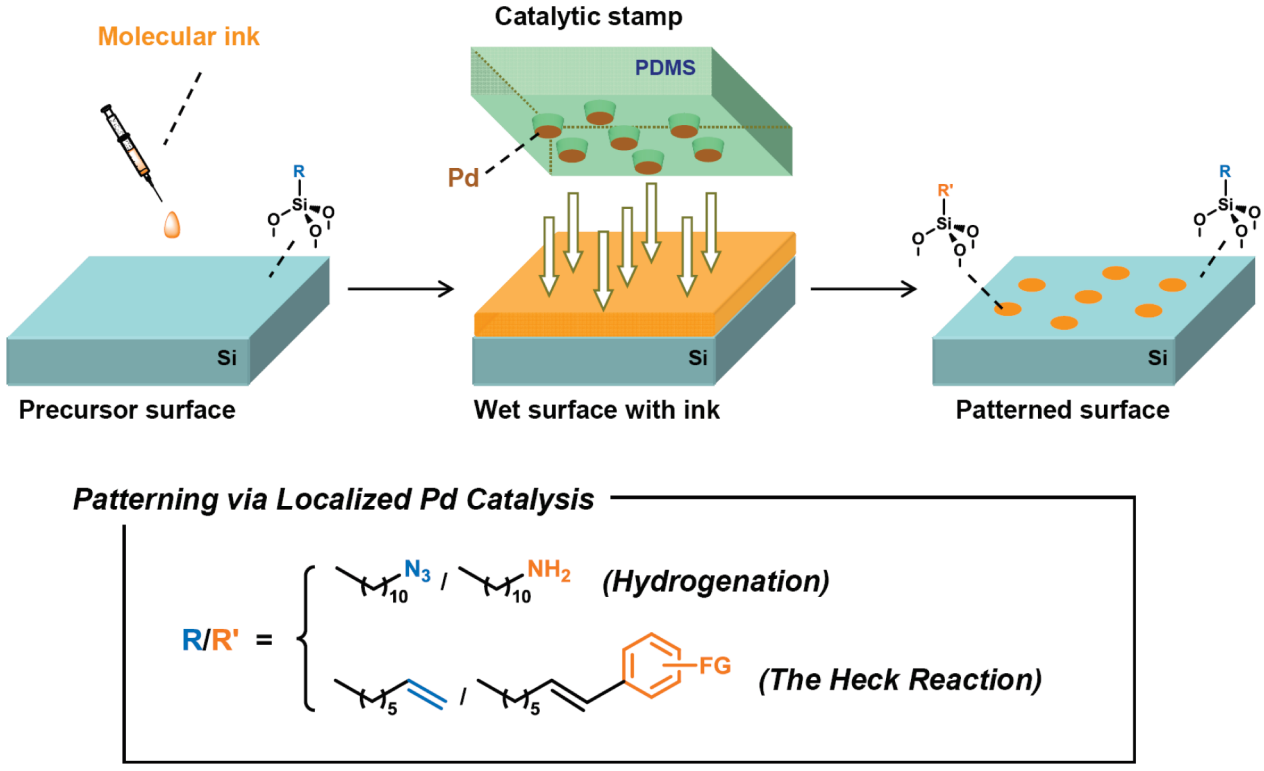

[a] A Pd catalytic stamp was applied directly onto an inked (wet) precursor surface. After stamping under given conditions, a molecular nanoarray was produced as a result of localized catalysis by immobilized Pd. Typical conditions: Stamping at room temperature for 5 min for hydrogenation, and for the Heck reaction, stamping was initiated at room temperature, and then heated to 130 °C for 30 min. FG = functional group.

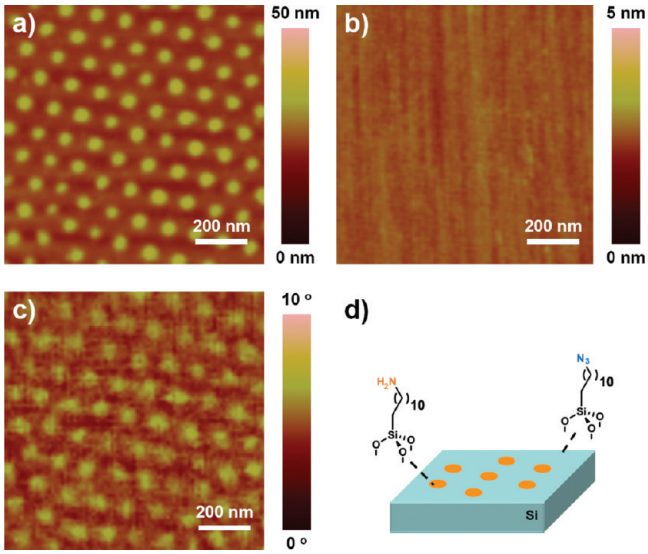

FIGURE 1. AFM images of a Pd catalytic stamp and a patterned azide-terminated surface following patterned catalytic hydrogenation. (a) Height image of a Pd catalytic stamp, whose Pd size is 33 nm and center-to-center spacing is 116 nm. (b) Height and (c) phase images of a patterned surface using the stamp shown in image a. (d) Cartoon schematic of the expected amine/azide-patterned surface.

procedures (16, 17). To obtain azide-terminated surfaces, we first assembled 11-bromoundecyltrichlorosilane on oxide-capped Si substrates, followed by nucleophilic substitution of the terminal Br functionalities by azide groups (16). In another unsaturated variation, alkene-terminated surfaces were directly prepared via the assembly of 7-octenyltrichlorosilane (17). It should be noted, in both cases, that the reaction conditions (vapor or solution phase) and the cleaning process following silane assembly need to be carried out with care to achieve high quality, smooth surfaces necessary for the following AFM analyses (see detailed Experimental Procedures in the Supporting Information).

Scheme 1outlines the general procedure for the nanoscale modification of organic monolayer surfaces using catalytic stamps. A freshly prepared precursor surface was covered with a solution of a molecular ink, and then a Pd catalytic stamp was applied onto the wet surface under ambient conditions. The stamping was continued under static pressure for a given time and temperature (5 min and room temperature for hydrogenation, 30 min and 130 °C for the Heck reaction) in laboratory ambient. During this process, localized catalytic reactions proceeded exclusively underneath the immobilized Pd catalysts, and pattern broadening due to ink diffusion and stamp deformation did not occur. As a result, the subsequent release of the Pd catalytic stamp led to the accurate translation of catalyst patterns into molecular patterns, depending upon the reactions used. Amine groups were generated from azide-terminated surfaces by hydrogenation, whereas aryl groups with different functionalities were attached onto alkene-terminated surfaces via the Heck reaction. After extensive washing, the resulting sample underwent a series of analyses (vide infra).

Hydrogenation of surface azide groups (16, 18) was carried out using a saturated 2-propanol solution of H_2 (gas) as the molecular ink. Shown in Figure 1 is the tapping mode atomic force microscope (AFM) images of a parent Pd

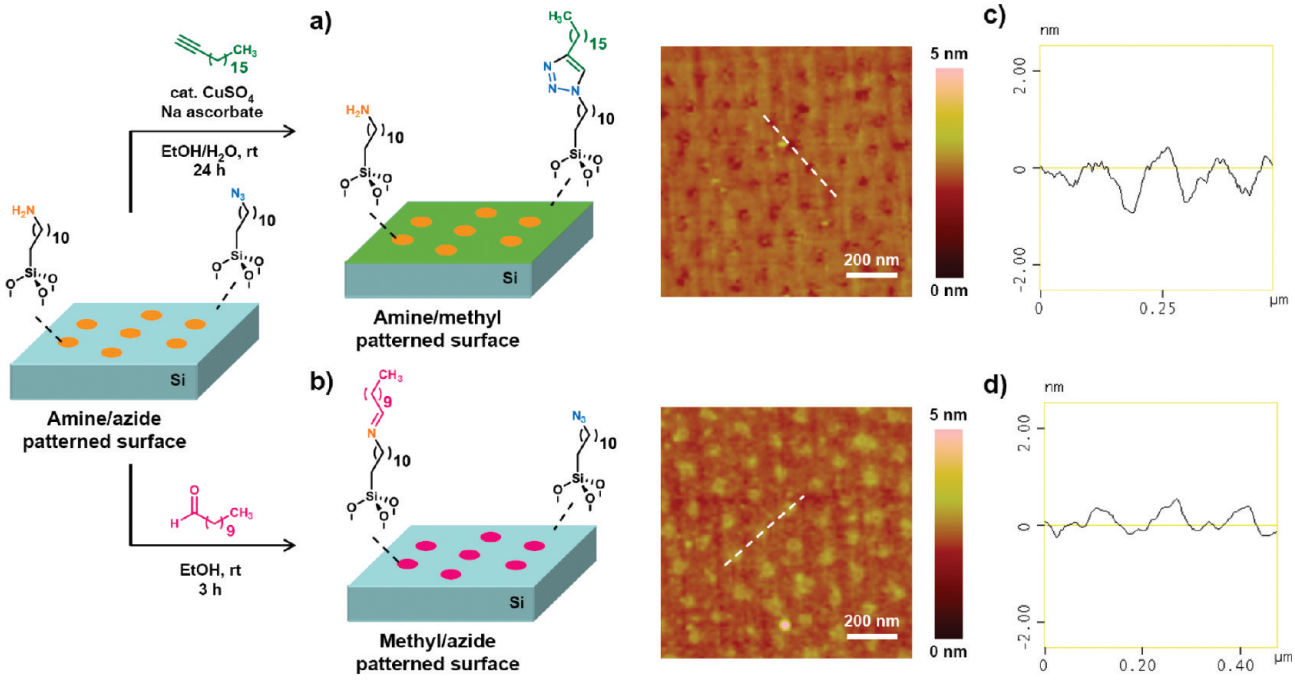

FIGURE 2. Outline for the chemical modification of an amine/azide-patterned surface, including AFM images and height profile data. (a) Amine/methyl-patterned surface obtained through Cu^{I}-catalyzed azide−alkyne cycloaddition. (b) Methyl/azide-patterned surface obtained through imine formation. (c, d) Height profiles of dashed line in AFM images a and b, respectively.

catalytic stamp and a stamped azide-terminated surface. The average domain size and center-to-center spacings of the hexagonally patterned Pd nanostructures were 33 and 116 nm, respectively (Figure 1a). Because of the subtle difference in heights (<0.2 nm) between the original azide and the newly formed amine groups, no topographic features were detected in the height-mode AFM image (Figure 1b). In the phase image, however, a hexagonally patterned dot array, with nearly identical domain size and center-to-center spacing of the parent catalytic stamp, was observed (Figure 1c). The positive (brighter) features result from the attractive interaction between the modified domains and the oxide-capped silicon cantilever (15), implying formation of hydrophilic amine functionalities by catalytic stamping (Figure 1d).

To examine the chemical details of the resulting patterned surface, X-ray photoelectron spectroscopy (XPS) was then carried out. No significant contamination from the Pd catalyst was detected in the Pd(3d) region within the limits of this technique (see the Supporting Information, Figure S1a) (19). High-resolution XPS spectra of the N(1s) region was also examined by comparing with the original azide-terminated surface (before stamping, Supporting Information, Figure S1b) (20). Although a decrease in the peak area around 405 eV, compared to the larger feature at 400−402 eV, was observed upon patterning (Supporting Information, Figure S1c), it was still not convincing enough to substantiate the generation of amine groups, whose expected energy of ~400 eV would overlap with the azide groups (21).

Although the exact yield of the surface conversion was not spectroscopically traced using another technique (like Fourier transform infrared spectroscopy, for example), evidence for formation of the expected amine/azide-patterned surface was supplemented by demonstrating specific chemical modifications on both amine or azide groups (Figure 2). First, a selective reaction on the azide termination, Cu^{I}-catalyzed azide−alkyne 1,3-dipolar cycloaddition (CuAAC, click chemistry), was carried out (Figure 2a). When the stamped sample was treated with an ethanol/water (2/1, v/v) solution of 1-octadecyne (1 mM) containing a catalytic amount of $CuSO_4$ (10 μM) and sodium ascorbate (15 μM) for 24 h, the 1,3-dipolar cycloaddition between surface azide groups and 1-octadecyne proceeded (22). Although the original amine/azide patterned surface has no topographic features as mentioned previously (Figure 1b), the AFM height image of the reacted surface showed a pseudohexagonal array of nanoholes (Figure 2a), pointing to the successful attachment of 1-octadecyne molecules only on the azide-terminated regions. In the next step, the amine groups were selectively reacted with an aldehyde-containing molecule (Figure 2b). The stamped sample was immersed into an ethanol solution of undecanal (1 mM) for 3 h to link it to the amine-terminated moieties via imine formation (23). Because of the attachment of the long undecanyl chain, height growth was observed only on the hexagonally patterned amine-terminated domains. The section analyses of resulting AFM images showed that each nanohole (formed via click chemistry) or nanodomain (formed via imine formation) is approximately 1.3 nm deep (Figure 2c), or 0.7 nm tall (Figure 2d), respectively. Both these values are significantly less than the theoretically calculated numbers (see the Supporting Information, Figure S2); assuming an upright orientation with entirely trans configurations of the methylene groups (the maximum possible height), the expected depth of the nanoholes would be ~2.3 nm, and the height of the nanodomains ~1.2 nm. The observation of thinner organic layers could be due to two factors. First, the AFM

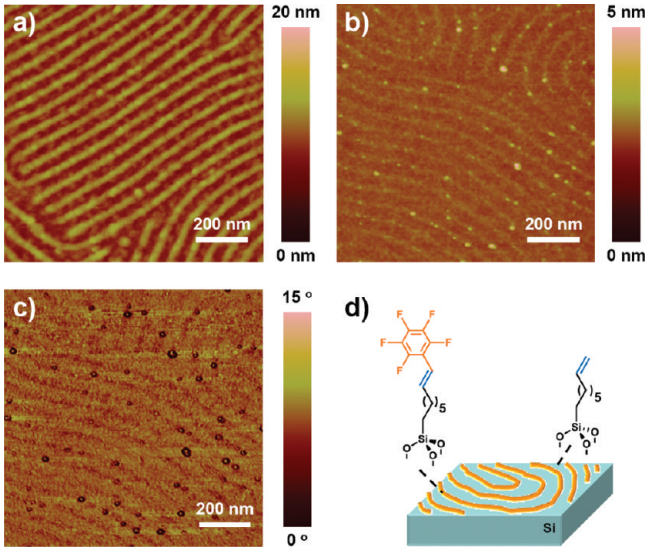

FIGURE 3. AFM images of a Pd catalytic stamp and an iodopentafluorobenzene-stamped alkene-terminated surface (Heck reaction). (a) Height image of a linearly patterned Pd catalytic stamp, with a measured line width of 15 nm and line-to-line spacing of 59 nm. (b) Height and (c) phase images of the patterned surface. (d) Cartoon schematic of the expected pentafluorobenzene/alkene-patterned surface.

tip pressure will result in some compression (24), and second, the created features are most likely tilted and loosely packed (i.e., imperfect conversion), probably because of the heterogeneous nature of surface reactions (25).

Demonstration of nanoscale patterning with hydrogenation-based catalytic stamping was followed by the investigation of a carbon−carbon bond forming reaction on alkene-terminated surfaces (the Heck reaction) (26). Although hydrogenation allowed a simple monofunctional transformation (azide to amine), more versatile modifications should be feasible by the Heck reaction. As the proof-of-principle for the molecular inks, a diluted dimethylformamide (DMF) solution of an aryl iodide (2.5 mM) containing triethylamine (2.5 mM) was employed, under phosphine-free conditions (26a, 27); these conditions were explored to avoid an excessive quantity of reagents at the catalyst/ink/alkene interface upon stamping. Figure 3 shows tapping-mode AFM images of a Pd catalytic stamp and a stamped alkene-terminated surface. The Pd nanostructure of the parent catalytic stamp was 15 nm in domain size (line width) and 59 nm in center-to-center (line-to-line) spacing (Figure 3a). When iodopentafluorobenzene (28) was stamped on an alkene-terminated surface, the formation of a similar linear pattern was observed as positive (brighter) features in the AFM height image (Figure 3b, height profile in Supporting Information, Figure S3). The incorporation of pentafluorophenyl groups was suggested by the AFM phase image (Figure 3c), because the more hydrophobic nature of the pentafluorophenyl groups compared to the surrounding alkene groups could be confirmed from the negative (darker) features recorded (15) (Figure 3d).

Figure 4 shows high-resolution XPS spectra obtained from the iodopentafluorobenzene-stamped sample. In the F(1s) region, a signal was observed at 693 eV (Figure 4a), again indicating incorporation of pentafluorophenyl groups (29) on the alkene-terminated surface. Because the spectrum in the Pd(3d) region showed no peaks around 335 eV (Figure 4b) (19), it was suggested that significant Pd leaching did not occur during the pattern formation, as seen in the case of hydrogenation-based catalytic stamping (vide supra). Other possible elements were also examined, and no detectable peaks were found from iodine derivatives (either iodopentafluorobenzene or the HI byproduct) (19) (see the Supporting Information, Figure S4a). Trace signals were observed, however, in the N(1s) region (19), indicating a minor contamination by DMF and/or triethylamine during the patterning process (see the Supporting Information, Figure S4b).

Another example of the Heck reaction-mediated patterning on the alkene-terminated surface is shown in Figure 5. A hexagonally patterned Pd catalytic stamp (the mean domain size and center-to-center spacing is 54 and 168 nm, respectively, Figure 5a) and a 4-iodoaniline-based molecular ink were employed in this case. The AFM images of the stamped surface revealed the formation of the hexagonal dot array both in height and phase modes (Figure 5b, c, respectively). While the theoretical height difference is calculated at ~0.5 nm, the measured value was ~0.4 nm, again due to the AFM tip compression and/or the loosely packed structure due to imcomplete conversion (see the Supporting Information, Figure S5). Because amine termina-

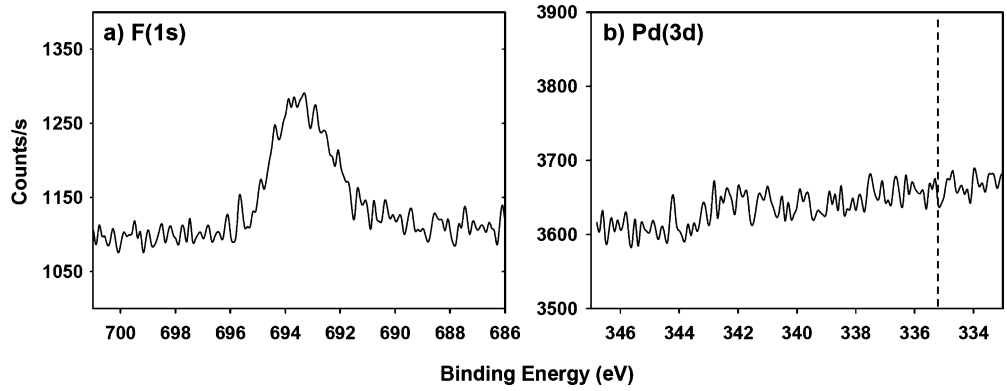

FIGURE 4. High-resolution XPS spectra of the (a) F(1s) and (b) Pd(3d) regions, obtained with the iodopentafluorobenzene-stamped sample (Heck reaction). The dashed line in (b) corresponds to elemental Pd (~335.4 eV).

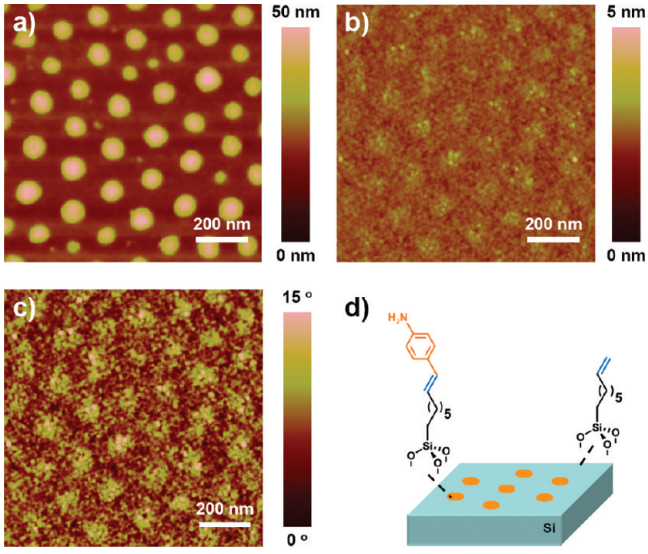

FIGURE 5. AFM images of a Pd catalytic stamp and a 4-iodoaniline-stamped alkene-terminated surface (Heck reaction). (a) Height-mode image of a hexagonally patterned Pd catalytic stamp with a domain size of 54 nm and center-to-center spacing of 168 nm. (b) Height and (c) phase images of the patterned surface. (d) Cartoon schematic of the expected amine/alkene-patterned surface.

tion is less hydrophobic than the alkene groups, the pattern appeared as an ensemble of positive features in the phase image (15).

The formed amine functionality was then probed by performing an amine-specific chemical reaction (Figure 6). As outlined in Figure 6a, the 4-iodoaniline-stamped sample was treated with a toluene solution of tetraoctylammonium bromide (TOAB)-capped Au nanoparticles (diameter ~5 nm) for 12 h. Because of ligand exchange between TOAB and surface amine groups (30), a hexagonally arranged pattern, consisting of clusters of gold nanoparticles, emerged after this treatment. The pronounced height difference was clearly observed by the AFM side-view images (Figure 6b, c). Scanning electron microscope (SEM) images further confirmed the selective deposition of gold nanoparticles into the expected hexagonal arrangement (Figure 6d, e).

Several control experiments were conducted for both hydrogenation and the Heck reaction to support the premise of pattern formations as a result of the corresponding catalytic reactions. For instance, when no H_2 (for hydrogenation) or aryl iodides (for the Heck reaction) was included in the molecular ink, patterned surfaces were not obtained. In addition, the use of azide- or alkene-free surfaces, such as native oxide-capped Si surfaces, resulted in no pattern formation. It was confirmed that high-temperature (130 °C) was necessary for the successful patterning by the Heck reaction, and when stamping was carried out at a lower temperature (110 °C), the resulting surface showed incomplete pattern formation (see the Supporting Information, Figure S6).

Reusability of stamps constitutes an important component of stamp-based lithography (15). The catalytic stamp used in hydrogenation was shown to be reusable multiple times (at least six times, see the Supporting Information, Figure S7). It was found, however, that no pattern could be produced once the catalytic stamps were used only

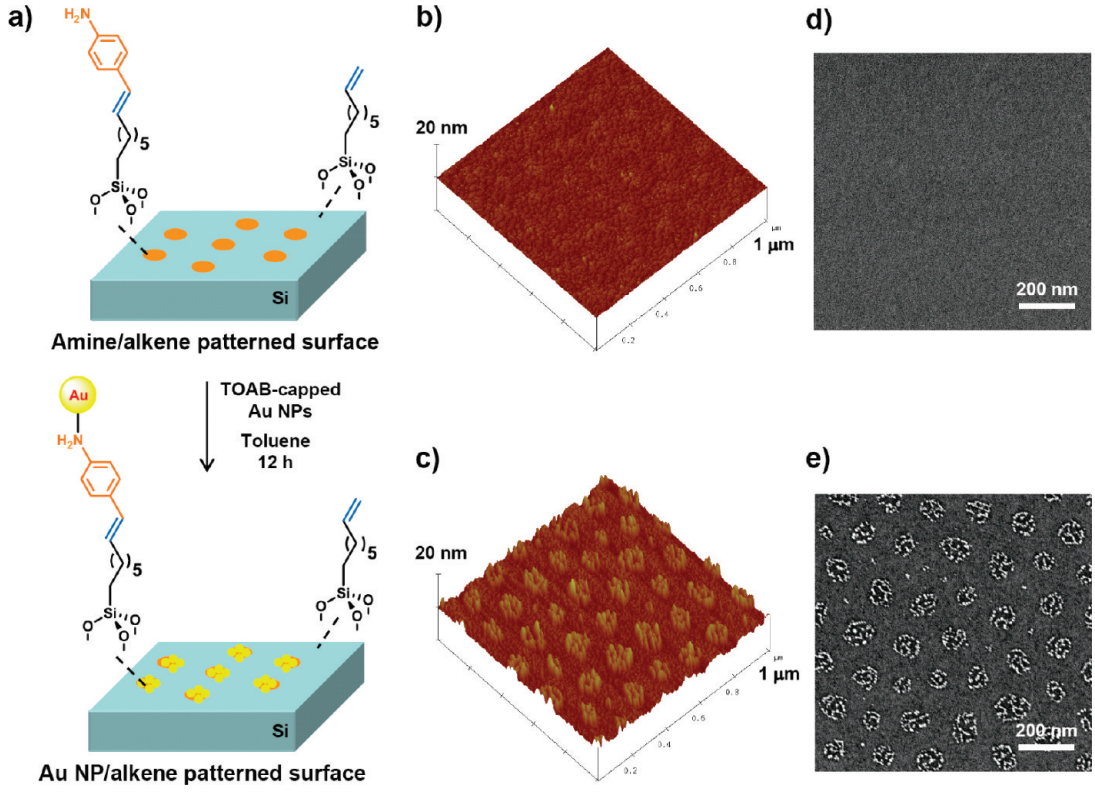

FIGURE 6. (a) Schematic outline for the assembly of TOAB-capped Au nanoparticles on the amine/alkene-patterned surface. AFM angled-view images of (b) a featureless, amine/alkene-patterned surface and (c) a hexagonally patterned Au nanoparticle/alkene-patterned surface. SEM images of (d) an amine/alkene-patterned surface and (e) a hexagonally patterned Au nanoparticle/alkene-patterned surface.

once in the Heck reaction. In the solution system, it is generally considered that catalytically active Pd species for the Heck reaction originated from leaching from solid Pd supports (31). Although the AFM image of a Pd catalytic stamp taken after use showed an identical appearance as the preuse state, a similar leaching mechanism from the Pd catalytic stamp might occur during the stamping. Indeed, the high resolution XPS spectrum of the stamped surface, taken immediately after the stamping (no washing), revealed a small quantity of Pd species on the surface (see the Supporting Information, Figure S8). Although the exact reason is unclear, the newly exposed Pd surface did not induce the Heck reaction, suggesting an inactive Pd species such as Pd black (31, 32). Post-treatment with $NaBH_4$ (aq) or Ar/H_2 plasma, however, could not retrieve any catalytic activity. A follow-up study is ongoing in our group to clarify the details in this respect.

CONCLUSION

A new extension of the contact printing-based sub-100 nm patterning approach, termed catalytic stamp lithography, on preformed organic monolayers, was demonstrated through the use of catalytic stamps. Azide- and alkene-terminated silane monolayers were prepared on oxide-capped Si substrates and used as precursor surfaces for hydrogenation and the Heck reaction, respectively. The generation of expected chemical functionalities was confirmed by AFM, XPS, and by site-selective modifications of stamped surfaces. Catalytic stamps could be reused multiple times for hydrogenation, but not for the Heck reaction, which provided an important insight on the selection of reactions available for the catalytic stamp-mediated patterning.

Acknowledgment. The authors thank the National Institute for Nanotechnology (NINT), Natural Science and Engineering Research Council (NSERC) of Canada, the National Research Council (NRC) Canada, the Canadian Foundation for Innovation (CFI), and the University of Alberta. The authors are also thankful for the technical support from the NINT (for SEM) and the Alberta Center for Surface Engineering and Science (for XPS).

Supporting Information Available: Detailed experimental procedures, additional AFM images, and XPS data. This material is available free of charge via the Internet at http://pubs.acs.org.

REFERENCES AND NOTES

(1) *Unconventional Nanopatterning Techniques and Applications*; Rogers, J. A.; Lee, H. H., Ed.; Wiley: Hoboken, NJ, 2009.
(2) (a) Barth, J. V.; Costantini, G.; Kern, K. *Nature* **2005**, *437*, 671–679. (b) Heath, J. R. *Annu. Rev. Mater. Res.* **2009**, *39*, 1–23.
(3) (a) Lin, H.-Y.; Chen, H.-A.; Lin, H.-N. *Anal. Chem.* **2008**, *80*, 1937–1941. (b) Arakaki, A.; Hideshima, S.; Nakagawa, T.; Niwa, D.; Tanaka, T.; Matsunaga, T.; Osaka, T. *Biotechnol. Bioeng.* **2004**, *88*, 543–546.
(4) (a) Har-Lavan, R.; Ron, I.; Thieblemont, F.; Cahen, D. *Appl. Phys. Lett.* **2009**, *94*, 0433081−0433083. (b) Hwang, E.; de Silva, K. M. N.; Seevers, C. B.; Li, J.-R.; Garno, J. C.; Nesterov, E. E. *Langmuir* **2008**, *24*, 9700–9706. (c) Grätzel, M. *Prog. Photovoltaics* **2006**, *14*, 429–442.
(5) (a) Truskett, V. N.; Watts, M. P. C. *Trends Biotechnol.* **2006**, *24*, 312–317. (b) Weibel, D. B.; DiLuzio, W. R.; Whitesides, G. M. *Nat. Rev. Microbiol.* **2007**, *5*, 209–218.
(6) (a) Ulman, A. *Chem. Rev.* **1996**, *96*, 1533–1554. (b) Love, J. C.; Estroff, L. A.; Kriebel, J. K.; Nuzzo, R. G.; Whitesides, G. M. *Chem. Rev.* **2005**, *105*, 1103–1169. (c) Hamers, R. J. *Annu. Rev. Anal. Chem.* **2008**, *1*, 707–736.
(7) (a) Salaita, K.; Wang, Y.; Fragala, J.; Vega, R. A.; Liu, C.; Mirkin, C. A. *Angew. Chem., Int. Ed.* **2006**, *45*, 7220–7223. (b) Mirkin, C. A. *ACS Nano* **2007**, *1*, 79–83.
(8) Huo, F.; Zheng, Z.; Zheng, G.; Giam, L. R.; Zhang, H.; Mirkin, C. A. *Science* **2008**, *321*, 1658–1660.
(9) (a) Geissler, M.; Bernard, A.; Bietsch, A.; Schmid, H.; Michel, B.; Delamarche, E. *J. Am. Chem. Soc.* **2000**, *122*, 6303–6304. (b) Delamarche, E.; Donzel, C.; Kamounah, F. S.; Wolf, H.; Geissler, M.; Stutz, R.; Schmidt-Winkel, P.; Michel, B.; Mathieu, H. J.; Schaumburg, K. *Langmuir* **2003**, *19*, 8749–8758. (c) Sharpe, R. B. A.; Burdinski, D.; Huskens, J.; Zandvliet, H. J. W.; Reinhoudt, D. N.; Poelsema, B. *J. Am. Chem. Soc.* **2005**, *127*, 10344–10349. (d) Coyer, S. R.; Garcia, A. J.; Delamarche, E. *Angew. Chem., Int. Ed.* **2007**, *46*, 6837–6840. (e) Duan, X.; Sadhu, V. B.; Perl, A.; Peter, M.; Reinhoudt, D. N.; Huskens, J. *Langmuir* **2008**, *24*, 3621–3627. (f) Zheng, Z.; Jang, J.-W.; Zheng, G.; Mirkin, C. A. *Angew. Chem., Int. Ed.* **2008**, *47*, 9951–9954.
(10) (a) Li, X. M.; Peter, M.; Huskens, J.; Reinhoudt, D. N. *Nano Lett.* **2003**, *3*, 1449–1453. (b) Snyder, P. W.; Johannes, M. S.; Vogen, B. N.; Clark, R. L.; Toone, E. J. *J. Org. Chem.* **2007**, *72*, 7459–7461. (c) Spruell, J. M.; Sheriff, B. A.; Rozkiewicz, D. I.; Dichtel, W. R.; Rohde, R. D.; Reinhoudt, D. N.; Stoddart, J. F.; Heath, J. R. *Angew. Chem., Int. Ed.* **2008**, *47*, 9927–9932.
(11) Li, H. W.; Muir, B. V. O.; Fichet, G.; Huck, W. T. S. *Langmuir* **2003**, *19*, 1963–1965.
(12) (a) Lin, M.-H.; Chen, C.-F.; Shiu, H.-W.; Chen, C.-H.; Gwo, S. *J. Am. Chem. Soc.* **2009**, *131*, 10984–10991. (b) Takakusagi, S.; Uosaki, K. *Jpn. J. Appl. Phys. 1* **2006**, *45*, 8961–8966. (c) Golzhauser, A.; Geyer, W.; Stadler, V.; Eck, W.; Grunze, M.; Edinger, K.; Weimann, T.; Hinze, P. *J. Vac. Sci. Technol., B* **2000**, *18*, 3414–3418.
(13) (a) Delamarche, E.; Schmid, H.; Bietsch, A.; Larsen, N. B.; Rothuizen, H.; Michel, B.; Biebuyck, H. *J. Phys. Chem. B* **1998**, *102*, 3324–3334. (b) Xia, Y.; Whitesides, G. M. *J. Am. Chem. Soc.* **1995**, *117*, 3274–3275. (c) Gannon, G.; Larsson, J. A.; Greer, J. C.; Thompson, D. *Langmuir* **2009**, *25*, 242–247.
(14) (a) Delamarche, E.; Schmid, H.; Michel, B.; Biebuyck, H. *Adv. Mater.* **1997**, *9*, 741–746. (b) Hui, C. Y.; Jagota, A.; Lin, Y. Y.; Kramer, E. J. *Langmuir* **2002**, *18*, 1394–1407. (c) Sharp, K. G.; Blackman, G. S.; Glassmaker, N. J.; Jagota, A.; Hui, C.-Y. *Langmuir* **2004**, *20*, 6430–6438.
(15) (a) Mizuno, H.; Buriak, J. M. *J. Am. Chem. Soc.* **2008**, *130*, 17656–17657. (b) Mizuno, H.; Buriak, J. M. *ACS Appl. Mater. Interfaces* **2009**, *1*, 2711–2720.
(16) Balachander, N.; Sukenik, C. N. *Langmuir* **1990**, *6*, 1621–1627.
(17) Kim, T. K.; Yang, X. M.; Peters, R. D.; Sohn, B. H.; Nealey, P. F. *J. Phys. Chem. B* **2000**, *104*, 7403–7410.
(18) (a) Muller, W. T.; Klein, D. L.; Lee, T.; Clarke, J.; McEuen, P. L.; Schultz, P. G. *Science* **1995**, *268*, 272–273. (b) Blackledge, C.; Engebretson, D. A.; McDonald, J. D. *Langmuir* **2000**, *16*, 8317–8323.
(19) Wagner, C. D.; Naumkin, A. V.; Kraut-Vass, A.; Allison, J. W.; Powell, C. J.; Rumble, J. R. *NIST X-ray Photoelectron Spectroscopy Database, NIST Standard Reference Database 20*, version 3.5; National Institute of Standards and Technology: Gaithersburg, MD, 2007; http://srdata.nist.gov/xps/.
(20) Prakash, S.; Long, T. M.; Selby, J. C.; Moore, J. S.; Shannon, M. A. *Anal. Chem.* **2007**, *79*, 1661–1667.
(21) Mengistu, T. Z.; Goel, V.; Horton, J. H.; Morin, S. *Langmuir* **2006**, *22*, 5301–5307.
(22) Lummerstorfer, T.; Hoffmann, H. *J. Phys. Chem. B* **2004**, *108*, 3963–3966.
(23) Rozkiewicz, D. I.; Ravoo, B. J.; Reinhoudt, D. N. *Langmuir* **2005**, *21*, 6337–6343.
(24) Zhiguo, L.; Zhuang, L.; Gang, W.; Yonghai, S.; Li, W.; Lanlan, S. *Microsc. Res. Technig.* **2006**, *69*, 998–1004.
(25) Gomez, M.; Li, J.; Kaifer, A. E. *Langmuir* **1991**, *7*, 1797–1806.
(26) (a) Davis, J. J.; Bagshaw, C. B.; Busuttil, K. L.; Hanyu, Y.; Coleman, K. S. *J. Am. Chem. Soc.* **2006**, *128*, 14135–14141. (b) Yam, C. M.; Cho, J.; Cai, C. *Langmuir* **2003**, *19*, 6862–6868. (c) Deluge, M.; Cai, C. *Langmuir* **2005**, *21*, 1917–1922. (d) Plass, K. E.; Liu, X.;

Brunschwig, B. S.; Lewis, N. S. *Chem. Mater.* **2008**, *20*, 2228–2233.
(27) Zhang, Z.; Wang, Z. *J. Org. Chem.* **2006**, *71*, 7485–7487.
(28) Albeniz, A. C.; Espinet, P.; Martin-Ruiz, B.; Milstein, D. *Organometallics* **2005**, *24*, 3679–3684.
(29) (a) Davis, D. W.; Shirley, D. A.; Thomas, T. D. *J. Am. Chem. Soc.* **1972**, *94*, 6565–6575. (b) Trudell, B. C.; Price, S. J. *Can. J. Chem.* **1977**, *55*, 1279–1284.
(30) (a) Thomas, K. G.; Zajicek, J.; Kamat, P. V. *Langmuir* **2002**, *18*, 3722–3727. (b) Prasad, B. L. V.; Stoeva, S. I.; Sorensen, C. M.; Klabunde, K. J. *Chem. Mater.* **2003**, *15*, 935–942.
(31) (a) Koehler, K.; Kleist, W.; Proeckl, S. S. *Inorg. Chem.* **2007**, *46*, 1876–1883. (b) Huang, L.; Wong, P. K.; Tan, J.; Ang, T. P.; Wang, Z. *J. Phys. Chem. C* **2009**, *113*, 10120–10130.
(32) Phan, N. T. S.; Van Der Sluys, M.; Jones, C. W. *Adv. Synth. Catal.* **2006**, *348*, 609–679.

AM100348F